3. Simpson, J. I., Graf, W. & Leonard, C. in *Progress in Oculomotor Research* (eds Fuchs, A. F. & Becker, W.) 475–484 (Elsevier, Amsterdam, 1981).
4. Graf, W., Simpson, J. I. & Leonard, C. S. Spatial organization of visual messages of the rabbit's cerebellar flocculus. II. Complex and simple spike responses of Purkinje cells. *J. Neurophysiol.* **60,** 2091–2121 (1988).
5. Wylie, D. R. & Frost, B. J. Responses of pigeon vestibulocerebellar neurons to optokinetic stimulation: II. The 3-dimensional reference frame of rotation neurons in the flocculus. *J. Neurophysiol.* **70,** 2647–2659 (1993).
6. Gibson, J. J. The visual perception of objective motion and subjective movement. *Psychol. Rev.* **61,** 304–314 (1954).
7. Lee, D. N. & Aronson, E. Visual proprioceptive control of standing in human infants. *Percept. Psychophys.* **15,** 529–532 (1974).
8. Owen, D. H. in *Perception & Control of Self-Motion* (eds Warren, R. & Fuchs, A. F.) 289–322 (Lawrence Erlbaum, Hillsdale, New Jersey, 1990).
9. Anderson, G. J. Perception of self-motion: psychophysical and computational approaches. *Psychol. Bull.* **99,** 52–65 (1986).
10. Krapp, H. G. & Hengstenberg, R. Estimation of self-motion by optic flow processing in single visual interneurons. *Nature* **384,** 463–466 (1996).
11. Duffy, C. J. & Wurtz, R. H. Sensitivity of MST neurons to optic flow stimuli. I. A continuum of response selectivity to large-field stimuli. *J. Neurophysiol.* **65,** 1329–1345 (1991).
12. Bradley, D. C., Maxwell, M., Anderson, R. A. & Banks, M. S. Mechanisms of heading perception in primate visual cortex. *Science* **273,** 1544–1547 (1996).
13. Wylie, D. R., Kripalani, T.-K. & Frost, B. J. Responses of pigeon vestibulocerebellar neurons to optokinetic stimulation: I. Functional organization of neurons discriminating between translational and rotational visual flow. *J. Neurophysiol.* **70,** 2632–2646 (1993).
14. Wylie, D. R. & Frost, B. J. Binocular neurons in the nucleus of the basal optic root (nBOR) of the pigeon are selective for either translational or rotational visual flow. *Vis. Neurosci.* **5,** 489–495 (1990).
15. Hess, B. J. & Dieringer, N. Spatial organization of linear vestibuloocular reflexes of the rat: responses during horizontal and vertical linear acceleration. *J. Neurophysiol.* **66,** 1805–1818 (1991).
16. Macpherson, J. M. Strategies that simplify the control of quadrupedal stance. I. Forces at the ground. *J. Neurophysiol.* **60,** 204–217 (1988).
17. Simpson, J. I. & Graf, W. in *Adaptive Mechanisms in Gaze Control: Facts and Theories* (eds Berthoz, A. & Melvill-Jones, G.) 3–16 (Elsevier, Amsterdam, 1985).
18. Soechting, J. F. & Flanders, M. Moving in three-dimensional space: frames of reference, vectors, and coordinate systems. *Annu. Rev. Neurosci.* **15,** 167–191 (1992).
19. Knudsen, E. I., du Lac, S. & Esterly, S. D. Computational maps in the brain. *Annu. Rev. Neurosci.* **10,** 41–65 (1987).
20. Jay, M. F. & Sparks, D. L. Auditory receptive fields in primate superior colliculus shift with changes in eye position. *Nature* **309,** 345–347 (1984).
21. Masino, T. & Knudsen, E. I. Horizontal and vertical components of head movement are controlled by distinct neural circuits in the barn owl. *Nature* **345,** 434–437 (1990).

Acknowledgements. We thank M. Dawson, D. Crewther and I. Curthoys for comments on this manuscript, and K. Lau and R. Glover for technical assistance. This research was supported by grants from the NSERC and AHFMR (to D.R.W.W.).

Correspondence and requests for material should be addressed to D.R.W.W. (e-mail: dwylie@psych.ualberta.ca).

Sniffing and smelling: separate subsystems in the human olfactory cortex

N. Sobel*, V. Prabhakaran*, J. E. Desmond†, G. H. Glover‡, R. L. Goode§, E. V. Sullivan*‖ & J. D. E. Gabrieli*†

** Program in Neuroscience and Departments of † Psychology, ‡ Radiology, § ENT Surgery and ‖ Psychiatry & Behavioral Sciences, Stanford University, Stanford, California 94305, USA*
§ Palo Alto VA Hospital, Palo Alto, California 94305, USA

The sensation and perception of smell (olfaction) are largely dependent on sniffing, which is an active stage of stimulus transport and therefore an integral component of mammalian olfaction[1,2]. Electrophysiological data obtained from study of the hedgehog, rat, rabbit, dog and monkey indicate that sniffing (whether or not an odorant is present) induces an oscillation of activity in the olfactory bulb, driving the piriform cortex in the temporal lobe, in other words, the piriform is driven by the olfactory bulb at the frequency of sniffing[3–6]. Here we use functional magnetic resonance imaging (fMRI) that is dependent on the level of oxygen in the blood to determine whether sniffing can induce activation in the piriform of humans, and whether this activation can be differentiated from activation induced by an odorant. We find that sniffing, whether odorant is present or absent, induces activation primarily in the piriform cortex of the temporal lobe and in the medial and posterior orbito-frontal gyri of the frontal lobe. The source of the sniff-induced activation is the somatosensory stimulation that is induced by air flow through the nostrils. In contrast, a smell, regardless of sniffing, induces activation mainly in the lateral and anterior orbito-frontal gyri of the frontal lobe. The dissociation between regions activated by olfactory exploration (sniffing) and regions activated by olfactory content (smell) shows a distinction in brain organization in terms of human olfaction.

The brains of six subjects were scanned in an experiment that contrasted the sniffing of non-odorized clean air with lack of sniffing. Sniffing induced activation primarily in the ventral temporal region (piriform, entorhinal and parahippocampal regions) and also in a small portion of the posterior and medial orbito-frontal cortex in all six subjects (Fig. 1a). Four subjects were then each rescanned four times; in each scan each subject was sniffing continuously at a different sniff-rate. Sniff-rate consistently determined the frequency of activity in the piriform cortex in all 16 scans (Fig. 2). Including the control experiments described below, sniff-induced activation occurred in the piriform of all 13 subjects tested. In 11 of the 13 subjects, sniff-induced activation was greater in the left piriform than in the right piriform (85% of subjects, $P < 0.02$).

In six additional experiments, we asked which sniffing-associated factor caused the piriform activation. First, we asked whether the sniff-induced activation was related to the motor action of sniffing or to the somatosensory stimulation induced by sniffing. Four subjects were scanned while they were sniffing with their nostrils blocked (that is, they were unsuccessfully trying to sniff); this eliminated the somatosensory stimulation associated with sniffing but maintained the motor element of sniffing. Such attempts to sniff did not induce significant activation in the piriform in any of the four subjects (Fig. 3B, d).

The same four subjects were then scanned under conditions of artificial sniffing, in which non-odorized air was puffed into the nostrils at a flow, duration, and rate similar to that of a natural sniff. This procedure, which eliminated the motor action but maintained the somatosensory element of sniffing, induced significant activation in the piriform of all four subjects (Fig. 3B, c).

An additional subject was scanned three times while sniffing with a partial occlusion of the nostrils that left 2-, 4-, or 6-mm opening. The smaller opening was associated with increased motor effort and decreased flow, whereas the larger opening was associated with decreased motor effort and increased flow. An increase in unoccluded-nostril diameter was consistently accompanied by an increase of activation in the piriform; in other words activation was related to the somatosensory sensation of air flow.

To address the possibility that sniff-induced activation may have reflected an fMRI contrast artefact (because of the periodic change in air content surrounding the nasal passages), rather than brain activity, we tested four additional subjects while they were sniffing before and after applying a topical anaesthetic to the nasal passages. Subjects were given an anaesthetic combined with a nasal dilator which, taken together, increased air flow as measured by anterior rhinometry. If sniff-induced activation were an artefact of air flow, this procedure would increase sniff-induced activation. Three of the four subjects reported a slight numbing sensation in the nostrils (but see ref. 7). The anaesthesia markedly reduced sniff-induced activation in the three subjects who reported a reduction in sensation (compare Fig. 3Ba, b), but not in the subject who did not report a reduction in sensation. The anaesthesia did not affect the perception of odours by these subjects in a standard test of olfactory identification (The University of Pennsylvania Smell Identification Test)[8]. Thus, sniff-induced activation is not an artefact related to air flow, but is instead related to brain activity induced by the sensation of air flow.

To address further the issue of possible airflow artefacts, we

scanned patient OT1, a 35-year-old woman who had undergone resection of the nerves inervating the nasal passage. She sustained a loss of olfactory and trigeminal perception in the left, but not the right, nostril. Sniffing through the intact nostril induced significant activation in the piriform, whereas sniffing through the anosmic nostril did not (compare Fig. 3Aa, b). These results show that air flow *per se* does not induce activation in the piriform. Rather, intact nerves are necessary for this activation to occur.

Another explanation for sniff-induced brain activation is that, despite the use of active-charcoal-filtered air in these experiments, the activation was odorant-induced. If the stimulus-delivery system was contaminated, piriform activations could have been induced by an odorant rather than by sniffing. This possibility was ruled out by the second main experiment, in which we localized activation induced by olfactory content alone (smell) rather than by olfactory exploration (sniffing).

Eight subjects were repeatedly asked to determine whether any odorant was present during a scan. In these smelling tasks, the presence of odorant was alternated with the absence of odorant while sniff-rate was held constant as a baseline. Each subject was scanned twice with the pure olfactory odorants decanoic acid and vanillin. Subjects were between 89% and 100% (mean 96%) accurate in detecting odorant presence/absence. The presence of odorants induced large activations in the anterior and lateral

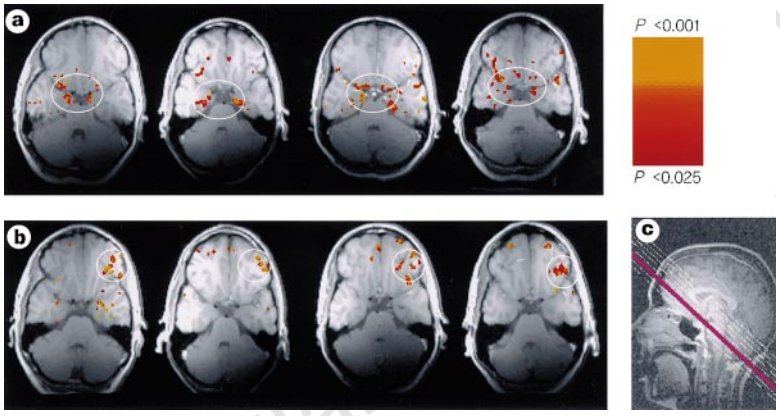

Figure 1 Brain regions activated by sniffing and smelling. **a**, The third slice (coloured purple in **c**) from four different subjects, showing sniff-induced activation primarily in the region of the piriform cortex in the temporal lobe and the medial and posterior orbito-frontal gyri in the frontal lobe (circled regions). **b**, The third slice in the same four subjects, showing activation induced by the presence of an odorant primarily in the lateral and anterior orbito-frontal gyri (circled regions). Odorant-induced activity was greater in the right than in the left lateral orbital gyrus ($t(7) = 2.49, P < 0.05$). **c**, Slice orientation. Locations within the oblique slices were cross-referenced to standard coronal slices[29,30]. Maximum activation induced by sniffing was at $x = -2.2$ cm, $y = 0.4$ cm, $z = -2.1$ cm, and by presence of odorant was at $x = 3$ cm, $y = 4.5$ cm, $z = -1$ cm.

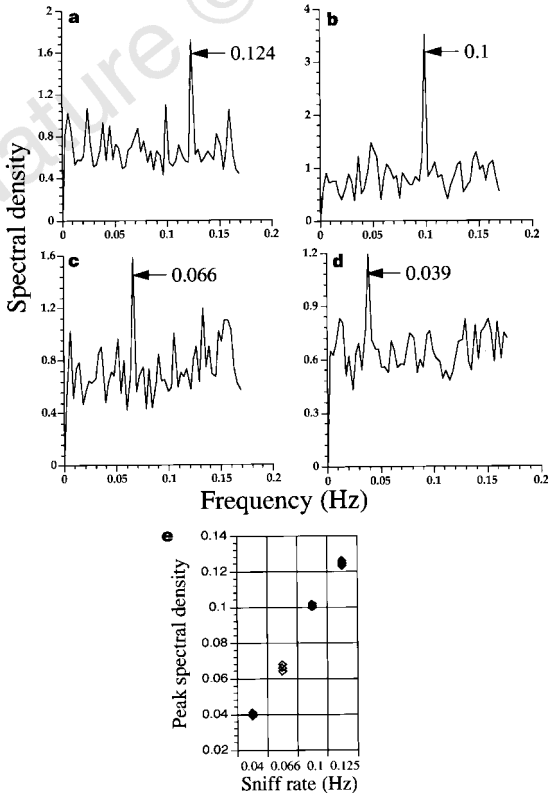

Figure 2 Fourier transform of activity within the temporal piriform during four different scans in the same subject. Subjects sniffed once every **a** 8 s (0.125 Hz), **b** 10 s (0.1 Hz), **c** 15 s (0.066 Hz) or **d** 25 s (0.04 Hz) in each scan. Sniffing frequency determined the frequency of activation in the piriform in each scan. **e**, This scatter diagram, representing the four subjects that participated in the control experiment, reveals the minimal variance in this effect. Respiration was monitored (0.38 Hz, 0.34 Hz, 0.30 Hz and 0.32 Hz in the four scans, respectively) in order to assure that overall respiration rate was not linked to sniffing rate.

orbito–frontal cortices primarily, and lesser activations in the piriform, in all 16 scans (Fig. 1b). Activity in the lateral orbito-frontal cortex was significantly greater in the right than in the left hemisphere in six of eight subjects. No activation occurred in additional 'sham' scans when no odorant was present. Thus, odorant-induced activation occurred primarily in brain regions that were different from those in which sniff-induced activation occurred, and sniff-induced activation was not related to odorant contamination of the system. (Odorant presence also induced activations in the peri-insular region, superior temporal, and various parts of the limbic system. Here, however, we focus on the dynamics of activity in the classic olfactory regions that occupy the ventral aspects of the brain.) The difference between sniff-induced and odorant-induced activation was seen in each subject simultaneously during the same scan (Fig. 4).

We have not determined which of several intranasal nerves convey the sniff-induced information. The somatosensory nature of the stimulus suggests that sniff-induced activation may be conveyed via the trigeminal nerve[9] (CNV 5). In some species, however, the olfactory receptors and nerve (CNV 1) convey not only odorants but also mechanical pressure[3,6]. Our results indicate that the human olfactory nerve may be mechanically sensitive. The role of sniff-induced activation in olfaction is unknown. Sniffing may be an attentional mechanism in olfaction. A sniff may, therefore, temporarily prime the piriform for the arrival of odour information, and may thus increase the probability of detecting odours in the olfactory system. Piriform activation is driven primarily by sniff rather than smell, but odour-content information may still be found in the piriform: odour information may be temporally coded in the nervous system[10]. If the odour information in the piriform is temporally coded, changes in odour content could change the order of neuronal firing, without altering overall firing rate. Such a difference in temporal codes of activity would be undetectable in this fMRI analysis.

The difference in brain-activity patterns induced by sniffing and smelling corresponds broadly with the localization of the primary and secondary olfactory cortices. At present the human primary olfactory cortex is thought to lie in the piriform cortex of the temporal lobe, and the secondary olfactory cortex is believed to lie in the orbito-frontal gyri of the frontal lobe and the insula of the temporal lobe[11–16]. This distinction concurs broadly with the structural connectivity of the olfactory system[17–19].

If the exploratory stage of olfactory processing (sniffing) delineates the primary olfactory cortex, the sniff-induced activations show that primary olfactory cortex extends from the ventral temporal piriform into a small region in the posterior and medial orbito-

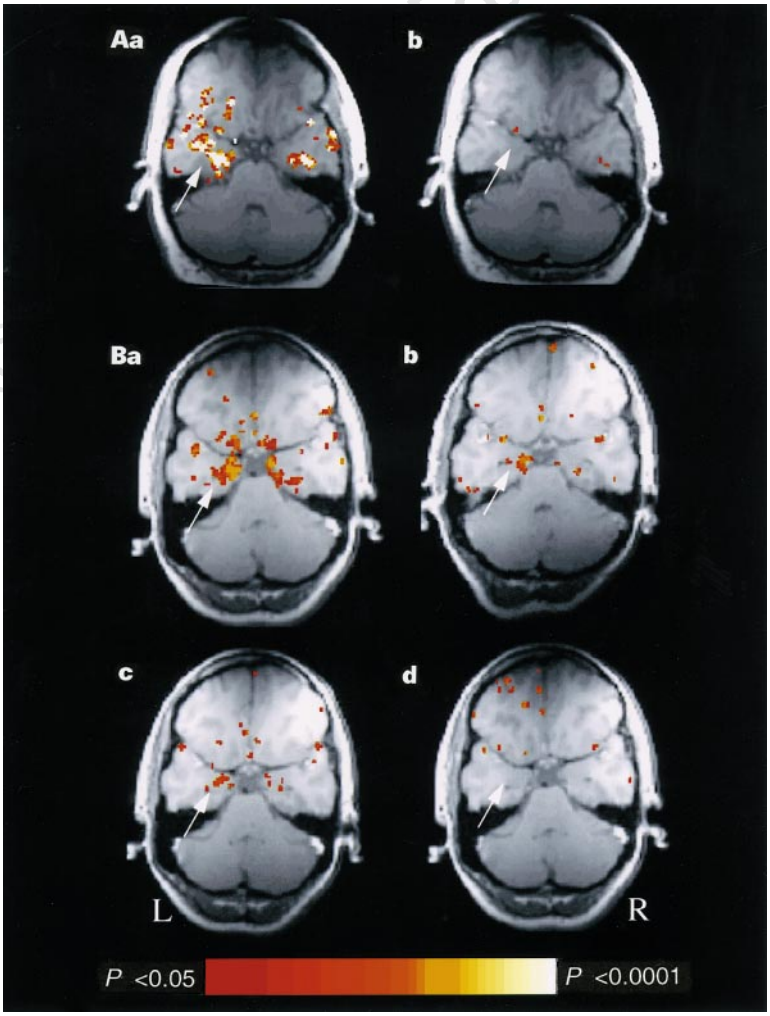

Figure 3 The component of sniffing that activates the piriform. **A,a**, Sniffing through the right, healthy, nostril in patient OT1. Piriform activation is evident. **b**, Sniffing through the left, anosmic, nostril in patient OT1. No significant activation is seen. **B,a**, Sniffing in healthy subject DP. Piriform activation is seen. **b**, Subject DP sniffing following anaesthesia. There is a reduction in activation in comparison with **a**. **c**, Subject DP lying passively while artificial sniffing occurs. Piriform activation is seen. **d**, Subject DP performing the motor action of sniffing with the nostrils occluded (that is, there is no air flow). No significant activation is seen. Arrows point to the region of the entorhinal and temporal piriform. R, right; L, left.

frontal cortex. This continuous region of activation may correspond with the cytoarchitectural extension of the piriform into the frontal lobe in humans[17,19]. Thus, in contrast to traditional views, primary olfactory cortex in humans may reside in both temporal and frontal lobes. If olfactory content (smelling) delineates the secondary olfactory cortex, the smell-induced activations specify the frontal-lobe portion of secondary olfactory cortex to the lateral and anterior orbito-frontal gyri (thus excluding the medial-posterior portions of the orbito-frontal cortex).

The role of sniffing in the dynamics of neural activity in the olfactory cortex may offer a new way to examine the olfactory deficits that are seen in many motor-neurodegenerative disorders[21–23]. The olfactory deficit in diseases such as Parkinson's disease[22] may be partly related to an inability to sniff rather than an inability to smell. Furthermore, the presence of both primary and secondary olfactory cortices within both frontal and temporal lobes may explain the diversity often seen in the extent and nature of olfactory deficits following temporal and frontal-lobe lesions[19,23,24]. □

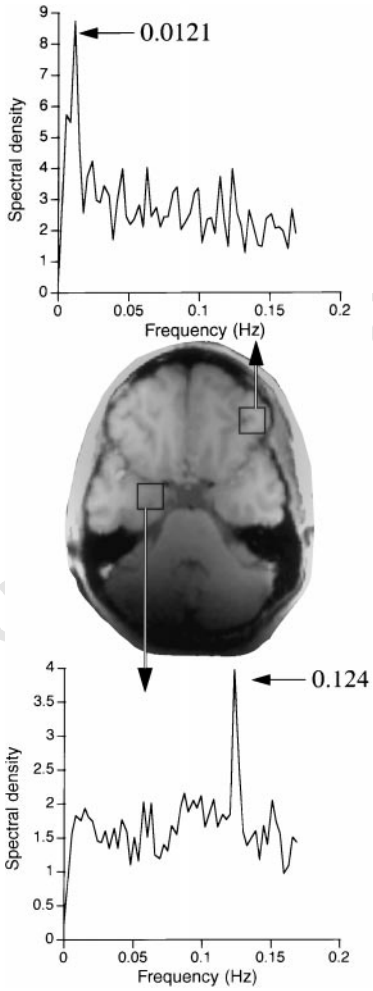

Figure 4 The dissociation between sniff-induced and odour-induced activity can be seen within the same subject at the same time (during the same scan). The subject performed a smell task (sniffing once every 8 s (0.125 Hz); odorant presence alternated with odorant absence every 40 s during the 320 s scan (0.0125 Hz)). Fourier transform of activity in the box marked in the piriform cortex (centre and bottom) and lateral orbito-frontal gyri (centre and top) reveals that whereas the primary frequency of activity in the former is determined by sniffing, activity in the latter is determined by smelling (odorant presence). In this image, the brain is seen to be performing two different tasks at two different frequencies simultaneously. Re-analysis of all the smelling tasks in all subjects at the frequency of sniffing also showed this effect.

Methods

Thirteen healthy subjects (seven women and six men, right-handed, non-smoking, mean age 28) and one unilaterally anosmic woman participated in the study. Odorant-generation methods are described in ref. 26. Odorant and no-odorant conditions were alternated, with a rise time of <500 ms, and were not associated with any auditory, visual, tactile or thermal cues.

Sniffing. During a scan, subjects viewed a screen via a mirror. An instruction was repeatedly projected to the screen every 8 s. Five repetitions of the instruction read "Sniff" and were followed by five repetitions reading "No sniff". The resulting cycle of 40 s sniffing followed by 40 s not sniffing was repeated four times, resulting in an experiment of 320 s. Subjects were instructed to maintain sniff duration while the message was projected, that is, for 1.5 s. In the somatosensory control experiments, subjects lay passively as clean air was puffed at the nostrils at 30 litres min^{-1} for 1.5 s, at the experimental rate. Anaesthesia was performed with topical application of phenylephrine hydrochloride (0.5%) followed by xylocaine (4%).

Smelling. An instruction reading "Sniff and respond, is there an odour? Press the right button for yes or the left button for no" was projected to the screen once every 8 s throughout the entire scan. The subject sniffed and then indicated response by using the index finger of the dominant hand to press one of two buttons. The instruction was presented at a constant rate (0.125 Hz), whereas 40 s odorant presence alternated with 40 s odorant absence four times, resulting in a 320-s experiment. Thus, the difference between the alternating conditions was restricted to the presence or absence of an odorant while sniffing was maintained as a constant subtracted baseline.

fMRI acquisition. Imaging was performed using a 1.5 T MRI scanner. A bite-bar was used to prevent head motion. Eight 4-mm-thick slices with a 2-mm interslice gap were acquired. Two 5-inch-diameter local-receive coils were used. A T2*-sensitive gradient echo spiral sequence[27] was used, with parameters of repetition time (TR) = 720 ms, echo time (TE) = 40 ms, flip angle = 65°, in-plane resolution = 2.75 mm^2, number of interleaves = 4, acquisition time = 2.88 s per frame, number of frames = 115. T1-weighted flow-compensated spin-warp anatomy images (TR = 500 ms, minimum TE) were acquired as a substrate on which to overlay functional data.

fMRI analysis. Methods of fMRI analysis are described in detail in refs 26, 28. Briefly, a reference function was computed by convolving a square wave at the task frequency (frequency of sniffing in the sniffing tasks or frequency of odorant presentation in the smelling tasks) with a data-derived estimate of the haemodynamic-response function. Correlations between the reference function and the pixel response time series were computed and normalized in a statistical parametric Z map[28]. Motion analysis was performed and corrected using an algorithm based on correlation of the image with a reference image.

Received 25 August; accepted 9 December 1997.

1. Le Magnen, J. Etude des facteurs dynamiques de l'excitation olfactive. *L'Année Psychologique* 77–89 (1945–1946).
2. Laing, D. G. Natural sniffing gives optimum odor perception for humans. *Perception* **12,** 99–117 (1983).
3. Adrian, E. D. Olfactory reactions in the brain of the hedgehog. *J. Physiol.* **100,** 459–473 (1942).
4. Bressler, S. L. & Freeman, W. J. Frequency analysis of olfactory system EEG in cat, rabbit, and rat. *Electro. Clin. Neurophysiol.* **50,** 19–24 (1980).
5. Bressler, S. L. Relation of olfactory bulb and cortex. II. Model for driving of cortex by bulb. *Brain Res.* **409,** 294–301 (1987).
6. Ueki, S. & Domino, E. F. Some evidence for a mechanical receptor in olfactory function. *J. Neurophysiol.* **24,** 12–25 (1961).
7. Jones, A. S., Lancer, J. M., Shone, G. R. & Stevens, J. C. The effect of lignocaine on nasal resistance and nasal sensation of airflow. *Acta Otolaryngol.* (Stockh.) **101,** 328–330.
8. Doty, R. L., Shaman, P. & Dann, M. Development of the University of Pennsylvania smell identification test: a standardized microencapsulated test of olfactory function. *Physiol. Behav.* **32,** 489–502 (1984).
9. Jones, A. S., Wight, R. G., Crosher, R. & Durham, L. H. Nasal sensation of airflow following blockade of the nasal trigeminal afferents. *Clin. Otolaryngol.* **14,** 285–289 (1989).
10. Wehr, M. & Laurent, G. Odour encoding by temporal sequences of firing in oscillating neural assemblies. *Nature* **384,** 162–166 (1996).
11. Price, J. L. in *The Human Nervous System* (ed. Paxinos, G.) 979–1001 (Academic, San Diego, 1990).
12. Price, J. L. *et al.* in *Olfaction, a Model System for Computational Neuroscience* (eds Davis, J. L. & Eichenbaum, H.) 101–120 (MIT Press, Cambridge, MA, 1991).
13. Zatorre, R. J. & Jones-Gotman, M. Right-nostril advantage for discrimination of odors. *Percept. Psychophys.* **47,** 526–531 (1990).
14. Zatorre, R. J. & Jones-Gotman, M. Human olfactory discrimination after unilateral frontal or temporal lobectomy. *Brain* **114,** 71–84 (1991).
15. Zatorre, R. J., Jones-Gotman, M., Evans, A. C. & Meyer, E. Functional localization and lateralization of human olfactory cortex. *Nature* **360,** 339–341 (1992).
16. Jones-Gotman, M. & Zatorre, R. J. Olfactory identification deficits in patients with focal cerebral excision. *Neuropsychologia* **26,** 387–400 (1988).

17. Allison, A. C. The secondary olfactory areas in the human brain. *J. Anat.* **88,** 481–488 (1954).
18. Potter, H. & Nauta, W. J. H. A note on the problem of olfactory associations of the orbitofrontal cortex in the monkey. *Neuroscience* **4,** 361–367 (1979).
19. Von Bonin, G. & Green, J. R. Connections between orbital cortex and the diencephalon in the macaque. *J. Comp. Neurol.* **92,** 243–254 (1949).
20. Eslinger, P. J., Damasio, A. R. & Van Hoesen, G. W. Olfactory dysfunction in man: anatomical and behavioral aspects. *Brain Cognit.* **1,** 259–285 (1982).
21. Elian, M. Olfactory impairment in motor neuron disease: a pilot study. *J. Neurol. Neurosurg. Psychiatr.* **54,** 927–928 (1991).
22. Doty, R. L., Deems, D. A. & Stellar, S. Olfactory dysfunction in Parkinsonism: a general deficit unrelated to neurologic signs, disease stage, or disease duration. *Neurology* **38,** 1237–1244 (1988).
23. Doty, R. L. *et al.* Olfactory dysfunction in three neurodegenerative diseases. *Geriatrics* **46** suppl 1, 47–51 (1991).
24. Potter, H. & Butters, N. An assessment of olfactory deficits in patients with damage to prefrontal cortex. *Neuropsychologia* **18,** 621–628 (1980).
25. Henkin, R. I., Comiter, H., Fedio, P. & O'Doherty, D. Defects in taste and smell recognition following temporal lobectomy. *Trans. Am. Neurol. Assoc.* **102,** 146–150 (1977).
26. Sobel, N. *et al.* A method for functional magnetic resonance imaging of olfaction. *J. Neurosci. Methods* **78,** 115–121 (1997).
27. Glover, G. H. & Lai, S. Self-navigated spiral fMRI: interleaved versus single-shot. *Magn. Reson. Med.* **39** (1998).
28. Friston, K. J., Jezzard, P. & Turner, R. Analysis of functional MRI time-series. *Hum. Brain Mapp.* **1,** 153–171 (1994).
29. Talairach, J. & Tournoux, P. *Co-planar Stereotaxic Atlas of the Human Brain* (Thieme, Stuttgart, 1988).
30. Desmond, J. E. & Lim, K. O. On- and offline Talairach registration for structural and functional MRI studies. *Hum. Brain Mapp.* **5,** 58–73 (1997).

Acknowledgements. This work was supported by the Stanford Program in Neuroscience (S.G.F.), Phil & Allen Trust, NIAAA, & NIMH. We thank L. Stryer, B. Wandell, D. Heeger, A. Pfefferbaum, G. Boynton, J. Demb, D. Peterson, G. Heit and J. Wine.

Correspondence and requests for materials should be addressed to N.S. (e-mail: nsobel@leland.stanford.edu).

Nocistatin, a peptide that blocks nociceptin action in pain transmission

Emiko Okuda-Ashitaka*, Toshiaki Minami†, Shinro Tachibana‡, Yoshihiro Yoshihara§‖, Yuji Nishiuchi¶, Terutoshi Kimura¶ & Seiji Ito*

** Department of Medical Chemistry, Kansai Medical University, Moriguchi 570, Japan*
Departments of † Anesthesiology and § Biochemistry, Osaka Medical College, Takatsuki 569, Japan
‡ School of Biological Sciences, The National University of Singapore, Singapore 119260, Singapore
‖ Department of Neuroscience, Osaka Bioscience Institute, Suita 565, Japan
¶ Peptide Institute Inc., Protein Research Foundation, Minoh 562, Japan

Prolonged tissue damage or injury often leads to chronic pain states such that noxious stimuli evoke hyperalgesia and innocuous tactile stimuli evoke pain (allodynia)[1,2]. The neuropeptide nociceptin[3,4], also known as orphanin FQ (ref. 5), is an endogenous ligand for the orphan opioid-like receptor[6–8] which induces both hyperalgesia and allodynia when administered by injection through the theca of the spinal cord into the subarachnoid space (that is, intrathecally)[4,9]. Here we show that the nociceptin precursor[3,10–13] contains another biologically active peptide which we call nocistatin. Nocistatin blocks nociceptin-induced allodynia and hyperalgesia, and attenuates pain evoked by prostaglandin E_2. It is the carboxy-terminal hexapeptide of nocistatin (Glu-Gln-Lys-Gln-Leu-Gln), which is conserved in bovine, human and murine species, that possesses allodynia-blocking activity. We have also isolated endogenous nocistatin from bovine brain. Furthermore, intrathecal pretreatment with anti-nocistatin antibody decreases the threshold for nociceptin-induced allodynia. Although nocistatin does not bind to the nociceptin receptor, it binds to the membrane of mouse brain and of spinal cord with high affinity. Our results show that nocistatin is a new biologically active peptide produced from the same precursor as nociceptin and indicate that these two peptides may play opposite roles in pain transmission.

Nociceptin is processed from its precursor prepronociceptin (Fig. 1). This sequence is bounded by pairs of the basic amino acids Lys-Arg, a general cleavage site for precursor maturation. The bovine nociceptin precursor protein consists of 176 amino acid residues. It contains three additional potential cleavage sites, delineating four processing products (bPNP-2, bPNP-3, bPNP-4 and bPNP-5), as shown in Fig. 1. The prepronociceptin gene[13] has organizational and structural features that are very similar to those encoding precursors of the endogenous opioid peptides preproenkephalin, preprodynorphin and prepro-opiomelanocortin. We therefore investigated the possibility that the nociceptin precursor might contain not only nociceptin but also an additional bioactive peptide(s) as maturation product(s).

To test whether these peptides are biologically active *in vivo*, we synthesized them chemically and investigated their effects on nociceptin-evoked pain responses in conscious mice. Simultaneous intrathecal (i.t.) injection of equal amounts of bPNP-3 and nociceptin (50 pg per mouse of each) significantly inhibited nociceptin-induced allodynia over the 50-min experiment. As shown in Fig. 2a, the allodynia caused by nociceptin was dose-dependently blocked by bPNP-3, with a half-maximal inhibitory dose (ID_{50}) (95% confidence limits) of 715 fg (34 fg–4.25 pg). However, bPNP-2, bPNP-4 and bPNP-5 did not affect allodynia at doses up to 500 pg. bPNP-3 (500 pg) did not induce allodynia by itself (not shown). Figure 2b shows the effect of synthetic peptides on nociceptin-evoked hyperalgesia by the hot-plate test. As compared with saline (17.6 ± 0.85 s, $n = 8$), nociceptin (50 pg) shortened the response latency to 8.7 ± 0.63 s, at 15 min after i.t. injection. The nociceptin-evoked hyperalgesia was significantly attenuated by 500 pg bPNP-3 and bPNP-4 (15.2 ± 1.03 s and 14.0 ± 0.31 s, respectively). The i.t. administration of bPNP-3 and bPNP-4 alone did not affect the latency period (not shown). Neither

Table 1 Inhibition of nociceptin-induced allodynia by peptides derived from bovine and mouse prepronociceptins

Species	Peptide	Sequence	ID_{50} (95% confidence limits) (pg)
Bovine	bPNP-3	TEPGLEEVGEIEQKQLQ	0.715 (0.034 – 4.25)
	bPNP-3-8P	EIEQKQLQ	0.125 (0.00096 – 1.33)
Mouse	mPNP-2/3	MPR-(35aa)-QLQ	1.80 (0.22 – 7.14)
	mPNP-3	AEPGADDAEEVEQKQLQ	2.33 (0.25 – 15.3)
	mPNP-3-8P	EVEQKQLQ	1.07 (0.034 – 8.07)
Conserved	PNP-3-6P	EQKQLQ	14.2 (6.29 – 47.1)
	PNP-3-6PΔN	QKQLQ	No inhibition at 500 pg
	PNP-3-6PΔC	EQKQL	No inhibition at 500 pg

Nociceptin (50 pg per mouse) was injected simultaneously with these synthetic peptides into conscious mice. Details are described in Methods. aa, Amino acids.

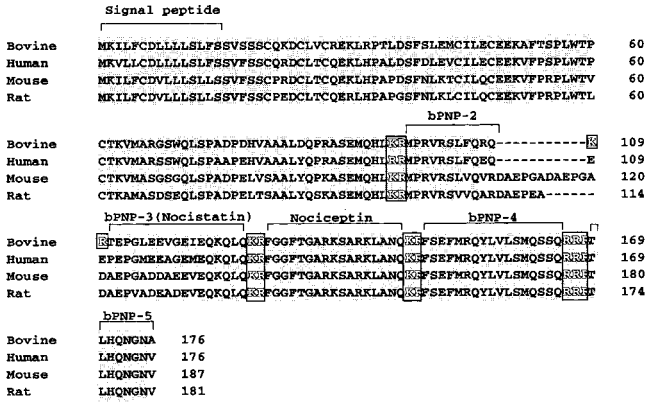

Figure 1 Alignment of deduced amino-acid sequences among bovine, human, mouse and rat prepronociceptins. Conserved amino acids are shaded and the putative proteolytic cleavage motifs are boxed. The signal peptide and putative peptides are indicated by overlines.